

## Case Report

# Dual-time points $^{18}\text{F}$ -FDG PET/CT imaging in detection of bone metastases from hepatocellular carcinoma

Xueren Zhao, Alex Yi, George Ariza, Lee Salcido

Department of Radiology, Loma Linda VA Hospital, 11201 Benton Street, Loma Linda, California 92357, USA

Received November 13, 2012; Accepted December 27, 2012; Epub January 26, 2013; Published February 6, 2013

**Abstract:** Bone scan is a well-established imaging modality in detection of osseous metastasis. However, its sensitivity decreases at evaluating lytic osseous metastasis in such entity as hepatocellular carcinoma (HCC). Increasingly, Fluorine-18 fluorodeoxyglucose positron emission tomography ( $^{18}\text{F}$ -FDG PET) with dual-time points imaging is utilized in detection of osseous metastasis from hepatocellular carcinoma. We report a case of HCC presenting with a focal increased activity on bone scan corresponding to left distal humeral fracture seen on an X-ray. Subsequent dual-time points  $^{18}\text{F}$  FDG PET/CT scan demonstrated interval increase in FDG activity involving the left distal humeral fracture, favoring neoplastic, rather than post fracture inflammatory process, later biopsy proven to be metastatic hepatocellular carcinoma. Several other FDG avid lesions were also found with interval increase in FDG activity on delayed images, helping to narrow the differential diagnosis to osseous metastases as a cause.

**Keywords:** Hepatocellular carcinoma, bone metastases, bone scan,  $^{18}\text{F}$ -FDG PET/CT, dual-time points imaging

## Case report

### Patient information

53 year old male with history of stage II hepatocellular carcinoma since October 2010 was treated with Sorafenib on April 7, 2011. The medication was stopped on April 3, 2012 due to disease progression. He reported sudden left arm pain on March 3, 2012 after carrying heavy water. The patient was found to have a spiral fracture through the distal left humeral diaphysis on an X-ray exam which also showed cortical thinning in the distal left humerus. Pathologic fracture was suspected. Whole body bone scan with 23 mCi Tc-99m hydroxymethylene diphosphate (HDP) was performed using Siemens T6 SPECT scanner 3 hours later and found a large solitary focus of intense radioactivity in the fracture site.

Non-contrast-enhanced  $^{18}\text{F}$ -FDG PET/CT images were obtained subsequently using Biograph Molecular PET/CT, Siemens. The patient was instructed to fast for 8 hours except for glucose-free oral hydration before the PET/CT examination. Blood glucose level prior to  $^{18}\text{F}$ -

FDG injection was 90 mg/dl. Intravenous injection of 474 MBq (12.8 mCi) of  $^{18}\text{F}$ -FDG was subsequently administered. The initial non-enhanced CT scan was performed from the skull base through the mid-thigh on 64-slice CT scanner using the following parameters: 120 kVp; 35 mA, with radiation exposure CTDI volume 9.7 mGy and DLP 982 mGycm. The delayed scan was only obtained of the chest and of the left elbow with CTDI volume 11.3 mGy and 430 mGycm. PET imaging was acquired in three dimensional mode at 2 minutes per bed position with the same scan range as the CT scan. SUV max was used to measure the FDG intensity. Dual-time points imaging technique with 2 hours separation was used to differentiate malignant uptake from post traumatic inflammatory uptake.

## Result

Bone scan revealed a large focus of intense radioactivity involving the left distal humeral fracture. No other osteoblastic metastatic lesions were identified (**Figure 1**).

$^{18}\text{F}$ -FDG PET/CT images revealed 8 FDG avid foci while bone scan demonstrated only one

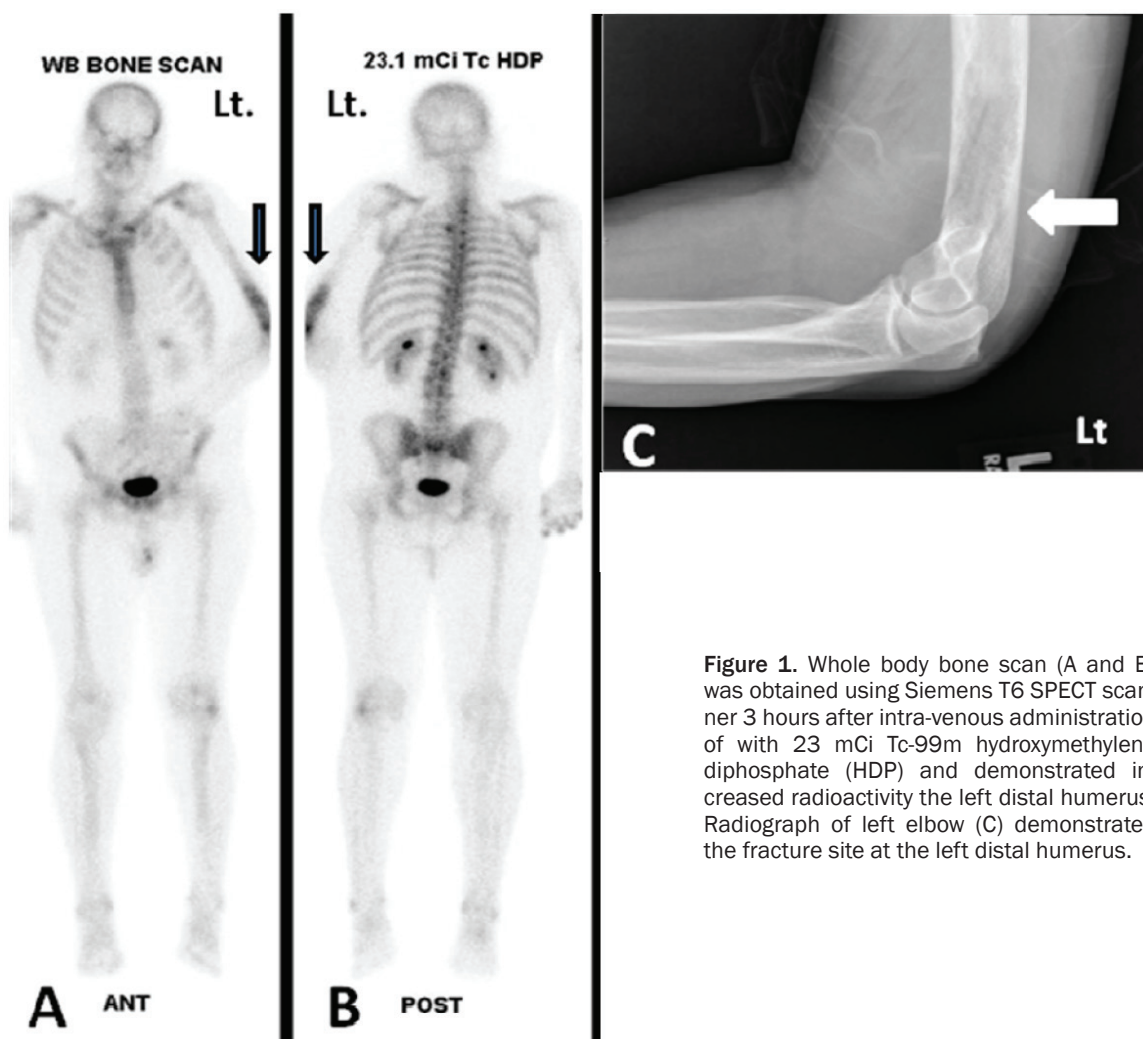


**Figure 1.** Whole body bone scan (A and B) was obtained using Siemens T6 SPECT scanner 3 hours after intra-venous administration of with 23 mCi Tc-99m hydroxymethylene diphosphate (HDP) and demonstrated increased radioactivity the left distal humerus. Radiograph of left elbow (C) demonstrated the fracture site at the left distal humerus.

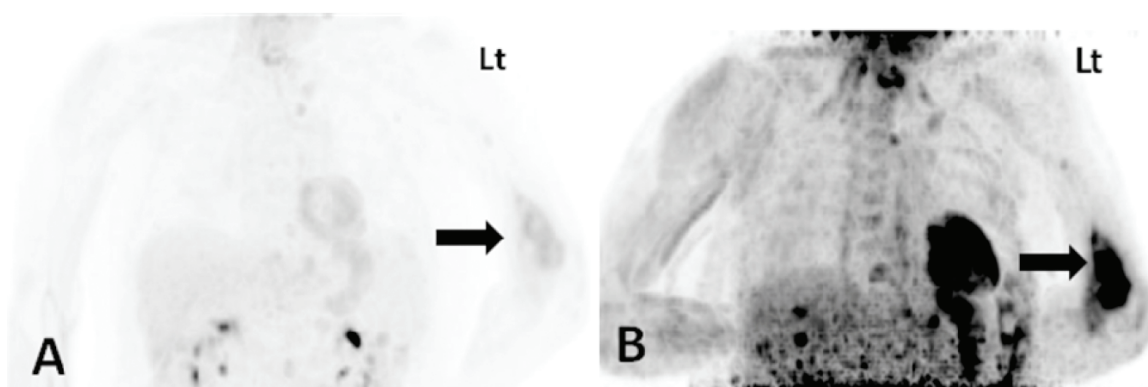


**Figure 2.** Initial PET image (A) shows increased FDG activity at left distal humeral fracture site with SUV max of 7. Delayed image (B) reveals SUV max of 8.9 with an interval increase in FDG activity by 27%.

HDP avid focus in the left distal humeral fracture site. Of the 8 FDG avid foci, dual-time points SUV measurements were obtained in 4

specific locations: left humeral pathologic fracture, C7, T9 and T12 vertebral bodies. The left humeral fracture, T9 and T12 vertebral bodies

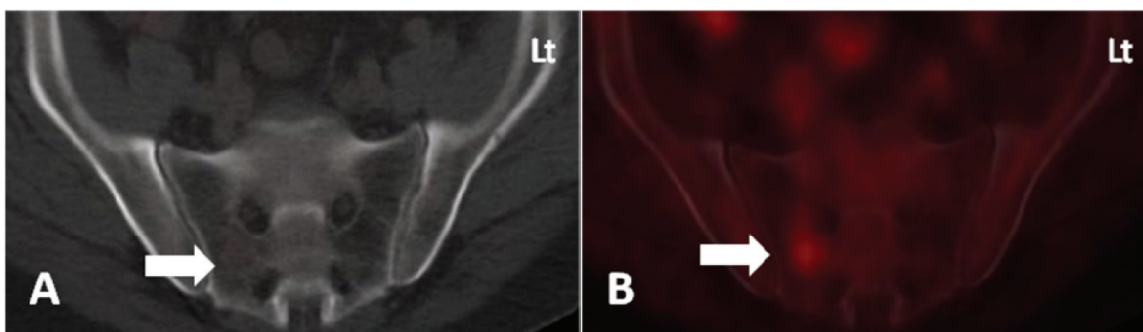


**Figure 3.** Non-contrast CT image (A) fails to show the osseous metastasis. Fused PET/CT image (B) shows a focus of increased FDG activity in the right inferior sacrum (SUV max 6.3).

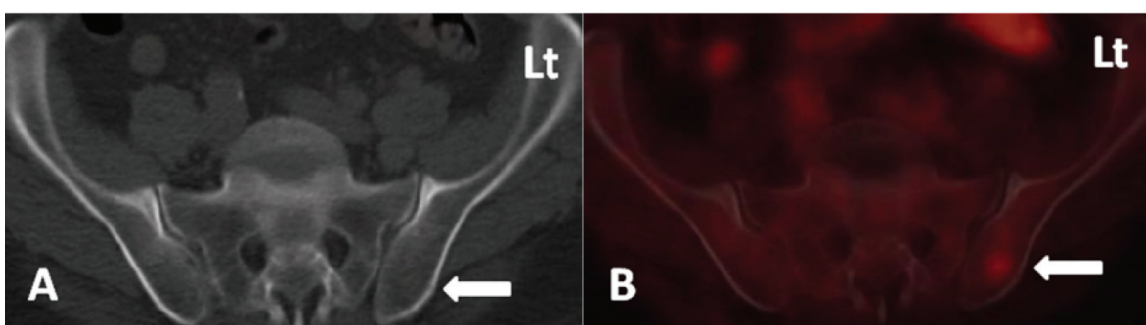


**Figure 4.** Non-contrast CT image of pelvis (A) fails to show the osseous metastasis in the left inferior ilium. Fused PET/CT (B) reveals a focus of increased FDG activity in the left inferior ilium (SUV max 4.6).

with associated lytic changes demonstrated more than 25% interval increase in FDG activity. The C7 vertebral bodies with associated soft tissue mass demonstrated only 5% interval increase in FDG activity on delayed imaging (Figure 2). Of other four FDG avid lesions in which dual-time points imaging were not obtained, one lesion (L5) demonstrated lytic change and three revealed no discernible osseous abnormality on the CT imaging of the study (false negative) (Figure 3, 4 and Table 1). Biopsy of left humeral <sup>18</sup>F-FDG avid lesion was performed on March 14, 2012 and confirmed moderately differentiated carcinoma positive for HepPar1, supporting osseous metastasis from hepatocellular primary carcinoma.

#### Discussion

Hepatocellular carcinoma (HCC) is the most common primary malignancy of the liver in adults and the third most common cause of cancer death worldwide. The incidence of HCC in the United States is rising steadily because of the prevalence of hepatitis C viral infection

and other causes of hepatic cirrhosis. It is currently the fifth most common solid tumor worldwide and the third leading cause of cancer-related death [1, 2]. The primary risk factor for HCC is liver injury from diverse causes that leads to hepatic cirrhosis in most patients. An estimated 78% of HCC cases and 57% of cases of liver cirrhosis are caused by chronic infection with hepatitis B virus (HBV) or hepatitis C virus (HCV) [3, 4]. Computed tomography (CT) and magnetic resonance imaging (MRI) are the current preferred modalities for imaging HCC [5, 6]. HCC tumors are optimally imaged using four-phase techniques, and these tumors typically demonstrate contrast enhancement in the arterial phase and washout of contrast media in the portal venous phase. <sup>18</sup>F-FDG PET has limited sensitivity for well-differentiated HCC due to low FDG uptake. However, <sup>18</sup>F-FDG PET has a relatively high detection rate (83%) for greater than 1 cm extra-hepatic metastases [7]. Delayed imaging at 2-3 hours after FDG injection may detect more metastatic lesion [8]. For instance, Sharma et al reported a study

## <sup>18</sup>F-FDG PET/CT imaging and bone metastases of hepatocellular carcinoma

**Table 1.** <sup>18</sup>F-FDG avid bone metastases in PET/CT versus Tc-99m HDP avid lesions in bone scan

Locations	<sup>18</sup> F-FDG PET/CT			Tc-99m HDP bone scan	CT bone window
	Initial	delayed	change %		
Lt. humerus	7.0	8.9	27%	Intensely uptake	Lytic change
C7	3.7	3.9	5%	negative	Lytic change and soft tissue formation
T9	3.5	4.5	29%	negative	lytic change
T12	3.4	5.5	32%	Negative	Lytic change
L5	6.3	N/A	N/A	negative	Lytic change
Lt. ilium	4.6	N/A	N/A	negative	negative
Rt. sacrum	6.3	N/A	N/A	negative	negative
Rt. acetabulum	5.5	N/A	N/A	negative	negative

of 48 pathologically confirmed HCC with extra-hepatic metastases and found <sup>18</sup>F-FDG PET/CT to be superior to conventional imaging (CT or MRI) in detection of metastatic lesions (37.5% versus 14.5%). The sensitivity, specificity, PPV and NPV of <sup>18</sup>F-FDG PET/CT for detecting metastases were 89.4%, 96.5%, 94.4%, 93.3% and that of CT were 27.7%, 93.3%, 71.4% and 68.2% respectively [9]. In a study of 4151 patients with hepatocellular carcinoma, Hyo Jung Seo et al reported that incidence of bone metastases from hepatocellular carcinoma was 6.3% (263/4151 patients) and <sup>18</sup>F-FDG PET/CT demonstrated higher detection rate of bone metastases than bone scan both in lesion-based analysis (sensitivity 98% vs 53%) and patient-based analysis (100% vs 80%) [10]. Delayed PET imaging may help to differentiate post traumatic inflammatory uptake from malignant lesion as malignant lesions usually demonstrate an increase in FDG uptake on 2-4 hour delayed images. FDG uptake usually reaches the peak level in 30 minutes in inflammatory process, whereas the maximum uptake occurs in 2-4 hours in malignant process [11, 12]. In our study, bone scan detected only one HDP avid lesion while FDG PET/CT identified 7 additional FDG avid lesions. Non-contrast CT study revealed corresponding osseous abnormality in 5 of 8 lesions (62.5%). Of the 4 FDG avid lesions with dual time points SUV measurements, 3 of 4 lesions (75%) with lytic bone change demonstrated interval increase in FDG uptake of more than 25% and one such lesion, the left distal humeral lesion, was biopsy proven to be bone metastasis from hepatocellular carcinoma. Only 1 of 4 lesions with soft tissue component demonstrated initial SUV max of 3.7 and interval FDG increase by 5% (SUV max 3.9). In the other 4 FDG avid lesions without

delayed imaging, CT imaging failed to detect abnormality in 3 of 8 lesions with 37.5% false negative detection rate. Our study suggests that <sup>18</sup>F-FDG PET may be superior to bone scan and to CT study in detection of bone metastases from hepatocellular carcinoma. Dual-time points <sup>18</sup>F-FDG PET/CT imaging technique may be helpful in differentiating the metastatic lesion from post traumatic inflammatory uptake.

**Address correspondence to:** Dr. Xueren Zhao, Radiology of Loma Linda VA Hospital, 11201 Benton Street, Room 4E-15, Loma Linda, California 92357, USA. Phone: 909-8257084, ext 2669; Fax: 909-7773204; E-mail: xueren.zhao@va.gov

### Reference

- [1] Jemal A, Ward E, Hao Y, Thun M. Trends in the leading causes of death in the United States, 1970-2002. *JAMA* 2005; 294: 1255-1259.
- [2] Bosch FX, Ribes J, Diaz M, Cléries R. Primary liver cancer: Worldwide incidence and trends. *Gastroenterology* 2004; 127: S5-S16.
- [3] Perz JF, Armstrong GL, Farrington LA, Farrington LA, Hutin YJ, Bell BP. The contributions of hepatitis B virus and hepatitis C virus infections to cirrhosis and primary liver cancer worldwide. *J Hepatol* 2006; 45: 529-538.
- [4] Chu CM, Liaw YF. Hepatitis B virus-related cirrhosis: Natural history and treatment. *Semin Liver Dis* 2006; 26: 142-152.
- [5] Kitamura T, Ichikawa T, Erturk SM, Nakajima H, Sou H, Araki T, Okada S, Enomoto N. Detection of hypervascular hepatocellular carcinoma with multidetector-row CT: Single arterial-phase imaging with computer-assisted automatic bolus-tracking technique compared with double arterial-phase imaging. *J Comput Assist Tomogr* 2008; 32: 724-729.
- [6] Kim MJ, Choi JY, Chung YE, Choi SY. Magnetic resonance imaging of hepatocellular carcinoma

## <sup>18</sup>F-FDG PET/CT imaging and bone metastases of hepatocellular carcinoma

- ma using contrast media. *Oncology* 2008; 75 suppl 1: 72-82.
- [7] Sugiyama M, Sakahara H, Torizuka T, Kanno T, Nakamura F, Futatsubashi M, Nakamura S. <sup>18</sup>F FDG PET in detection of extrahepatic metastases from hepatocellular carcinoma. *J Gastroenterol* 2004; 39: 961-968.
- [8] Ho CL, Chen S, Yeung DW, Cheng TK. Dual-Tracer PET/CT Imaging in the Evaluation of Metastatic Hepatocellular Carcinoma. *J Nuclear Med* 2007; 48: 902-909.
- [9] Sharma P, Singh H, Kumar R, Kumar R, Bal C, Malhotra A. Role of <sup>18</sup>F-FDG PET-CT for detection of extrahepatic metastasis in patients with hepatocellular carcinoma: Comparison with conventional imaging. *J nuclear medicine* 2011; 52 Supplement 1: 315.
- [10] Seo HJ, Choi YJ, Kim HJ, Jeong YH, Cho A, Lee JH, Yun M, Choi HJ, Lee JD, Kang WJ. Evaluation of Bone Metastasis from Hepatocellular Carcinoma Using <sup>18</sup>F-FDG PET/CT and <sup>99m</sup>Tc-HDP Bone Scintigraphy: Characteristics of Soft Tissue Formation. *Nucl Med Mol Imaging* 2011; 45: 203-211.
- [11] Lodge MA, Lucas JD, Marsden PK. A PET study of <sup>18</sup>F FDG uptake in soft tissue mass. *Eur J Nucl Med* 1999; 26: 22-30.
- [12] Lin WY, Tsai SC, Hung GU. Value of delayed <sup>18</sup>F-FDG PET imaging in detection of hepatocellular carcinoma. *Nucl Med Commun* 2005; 26: 315-321.